

High zinc sensitivity and pore formation in an invertebrate P2X receptor

Ramin Raouf, Dominique Blais, Philippe Séguéla*

Montreal Neurological Institute, Dept. Neurology and Neurosurgery, McGill University, 3801 University, Montreal, Que., Canada H3A 2B4

Received 15 November 2004; received in revised form 20 January 2005; accepted 20 January 2005

Available online 24 February 2005

Abstract

To investigate fast purinergic signaling in invertebrates, we examined the functional properties of a P2X receptor subunit cloned from the parasitic platyhelminth *Schistosoma mansoni*. This purinoceptor (SmP2X) displays unambiguous homology of primary sequence with vertebrate P2X subunits. SmP2X subunits assemble into homomeric ATP-gated channels that exhibit slow activation kinetics and are blocked by suramin and PPADS but not TNP-ATP. SmP2X mediates the uptake of the dye YO-PRO-1 through the formation of large pores and can be blocked by submicromolar concentrations of extracellular Zn^{2+} ions ($IC_{50}=0.4\text{ }\mu\text{M}$). The unique receptor phenotype defined by SmP2X suggests that slow kinetics, modulation by zinc and the ability to form large pores are ancestral properties of P2X receptors. The high sensitivity of SmP2X to zinc further reveals a zinc regulation requirement for the parasite's physiology that could potentially be exploited for therapeutic purposes.

© 2005 Elsevier B.V. All rights reserved.

Keywords: Purinoceptor; ATP; Cation channel; Ionotropic; *Schistosoma*; *Xenopus* oocytes

1. Introduction

The P2X family of receptor-channels mediates fast ionotropic responses to ATP. The different subtypes of P2X ATP-gated ion channels are homo- or heterotrimeric complexes generated by the specific assembly of seven homologous subunits in mammals (see [1] for review). Each P2X subunit displays two transmembrane domains separated by a large ectodomain with 10 conserved cysteines engaged in disulfide bridges, as well as intracellular amino- and carboxy-termini. From studies in heterologous expression systems and in native preparations, the vertebrate P2X receptors are grouped into three pharmacological categories: sensitive in the micromolar range to the agonist α,β -methyleneATP ($\alpha\beta\text{mATP}$) and to the non-competitive antagonist suramin (e.g. P2X1, P2X3,

P2X2+3), insensitive to $\alpha\beta\text{mATP}$ but sensitive to suramin (e.g. P2X2, P2X5), and insensitive to both (e.g. P2X4, P2X7). Structurally, the P2X gene family defines a distinct class of ion channels without a clear phylogenetic link to any other class of proteins so far. No P2X-related gene has been identified in the whole genomes of the model invertebrates *Drosophila*, *C. elegans* and *Plasmodium*, leaving the questions of the origin and evolution of these ion channels unanswered. There is evidence of actions of extracellular nucleotides in some invertebrates [2–4], however the status of fast purinergic signaling in these simpler organisms is unclear. Furthermore, a comparison of sequences and functional properties between evolutionarily distant P2X receptors will provide the basis for understanding the core structure–activity relationships of mammalian P2X receptors that are considered potential therapeutic targets. We describe here the specific functional phenotype of a member of the P2X family of ATP-gated receptor-channels isolated from the parasitic flatworm *Schistosoma mansoni*. During the preparation of this manuscript the cloning and character-

Abbreviations: BzATP, 2'-3'-O-(4-benzoylbenzoyl) ATP; $\alpha\beta\text{mATP}$, α,β -methyleneATP

* Corresponding author. Tel.: +1 514 398 5029; fax: +1 514 398 8106.

E-mail address: philippe.seguela@mcgill.ca (P. Séguéla).

ization of the same P2X receptor was reported by Agboh and collaborators [5]. Our results are in agreement with their findings. In addition, we report here the activation time course, zinc sensitivity, and ATP-mediated pore dilation.

2. Materials and methods

2.1. Molecular cloning

A BLAST search of the *S. mansoni* EST project identified the EST# CD081583 as part of the 3' region of a novel P2X subunit [6]. The novel P2X EST sequence was then used in rapid amplification of cDNA ends (RACE) to obtain the 5' end from a *S. mansoni* library (kindly provided by Dr. P. Ribeiro, McGill University). A set of exact match primers based on the RACE sequence and the EST was used in RT-PCR to amplify the full-length transcript from adult *S. mansoni* total RNA. A 1.4 kb PCR product was obtained and subcloned into pGEM-T vector. The clone containing a complete open reading frame was sequenced on both strands (Sheldon Biotechnology Center).

2.2. Functional expression and electrophysiology

The preparation of *Xenopus* oocytes for two-electrode voltage clamp recording has been described previously [7]. Defolliculated stage V or VI oocytes were injected with 60–100 ng of Smp2X cRNA (total volume 50 nL), 30 ng of mouse P2X7 cRNA or 0.9 ng of rat P2X2 cRNA. A two-electrode voltage clamp was carried out 24 to 96 h after injection. All drugs were dissolved in normal Ringer containing (in mM): 115 NaCl, 2.5 KCl, 5 NaOH, 10 HEPES. BaCl₂ (2mM) was used instead of CaCl₂ to prevent the activation of endogenous calcium-activated chloride currents. The oocytes were voltage-clamped at –60 or –120 mV unless otherwise stated. The data were digitized at 300 Hz and acquired using the Axodata software package. For current–voltage analysis, experiments were performed in ND96 Ringer containing (in mM) 96 NaCl, 2 KCl, 5 NaOH, 5 HEPES, and 2 BaCl₂. Voltage ramps from –60 to +40 mV (500 ms) were captured at 1 kHz.

2.3. YO-PRO-1 dye uptake

Oocytes injected with mouse P2X7 or Smp2X were washed with normal Ringer and incubated with normal divalent-free Ringer containing 10 μ M YO-PRO-1 (Molecular Probes) with or without 100–1000 μ M ATP for 10 min. The dye uptake was visualized using a Nikon TE300 Eclipse microscope equipped for epi-fluorescence. Images were acquired using a Sensicam CCD camera (Cooke) and the Axon Imaging Workbench software (Axon Instruments).

2.4. Data analysis

MacVector and GeneWorks softwares (Accelrys) were used for cDNA and protein sequence analysis. Current traces were analyzed using AxoGraph (Axon Instruments) and dose–response curves were constructed by fitting the Hill logistic equation using SigmaPlot. Fluorescence intensities in YO-PRO-1 uptake experiments were determined using the Jimage program (NIH). All data are presented as mean \pm standard error.

3. Results

3.1. Homology of Smp2X to mammalian P2X receptors

The complete open reading frame of the Smp2X clone was found to encode 437 residues (Genbank AY781699). At the nucleotide and protein level, significant homology with known P2X subunits unambiguously identifies this cDNA as an invertebrate P2X receptor subunit. We designated this P2X clone from *S. mansoni* as Smp2X in order to distinguish it from the putative P2X receptor from *Schistosoma japonicum* represented by EST# BU780470 in Genbank. Most conserved P2X structural motifs are present in Smp2X including the 10 extracellular cysteines, YXTXK/R in the N-terminus, as well as GF/YNFR and GXA/GGKF in the ectodomain (Fig. 1A). The amino acid sequence for Smp2X is most similar to the P2X4 and P2X5 subunits with 35% and 36% identity and 52% and 53% overall homology, respectively. However for any of the five predicted domains of the protein, i.e., the N-terminus, TM1, extracellular loop, TM2, and the C-terminus, the values of the homology with vertebrate subunits are similar (Fig. 1B). When only the ectodomain of the receptor is considered, the homology values vary from 50% with P2X3 to 61% with P2X5, suggesting similarities in agonist binding and gating (Fig. 1B). Smp2X is most divergent from the known P2X subunits in its C-terminus, also the region of least homology among members of the vertebrate P2X family (Fig. 1B).

3.2. Functional expression, pharmacology and ionic selectivity of Smp2X

Oocytes injected with Smp2X cRNA responded to the application of ATP with a slow-activating inward current (Fig. 2A). No desensitization was observed during subsaturating agonist applications, however at higher concentrations the current slowly desensitized (Fig. 2A). ATP evoked currents with an EC₅₀ of 13 ± 4 μ M (Hill coefficient $n=1.0 \pm 0.3$, Fig. 2B). Smp2X was more sensitive to agonist 2'-3'-O-(4-benzoylbenzoyl) ATP (BzATP) than ATP but was found to be nonresponsive to 100 μ M ADP, UTP or $\alpha\beta$ mATP (data not shown). At 10 μ M, purinergic antagonists suramin and PPADS

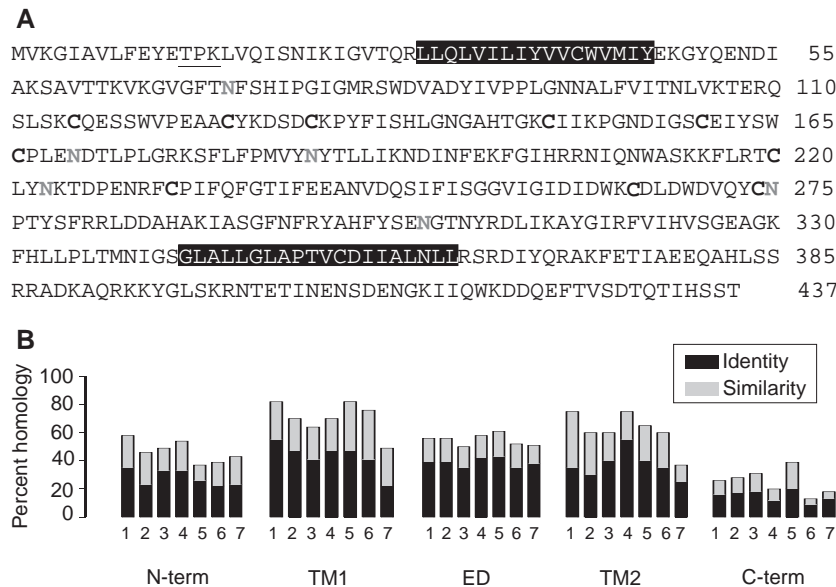


Fig. 1. Primary structure of SmP2X subunit. (A) Predicted amino acid sequence of the SmP2X cDNA. Boxed residues highlight the putative transmembrane (TM) domains. Residues in bold are conserved cysteines in all P2X family members, asparagine residues in grey correspond to putative glycosylation sites. A highly conserved PKC site in the N-terminal domain is underlined. (B) Homology of SmP2X with the rat subunits (P2X1-7) in the five main structural P2X domains. ED, ectodomain; TM, transmembrane domain.

blocked ATP currents by $79 \pm 4\%$ and $81 \pm 1\%$ respectively, but TNP-ATP was ineffective (Fig. 2C). The vertebrate P2X receptors identified so far are non-selective cation channels. The current–voltage (I–V) relationship for SmP2X exhibited little rectification in the voltage range analyzed (-60 to $+40$ mV) with a reversal potential of -3.0 ± 2 mV in the ND96 Ringer, suggesting that this receptor-channel is mainly selective for cations (Fig. 2D). The replacement of extracellular Na^+ with K^+ did not significantly change the reversal potential ($E_{\text{rev}} = 2 \pm 2$ mV, $P > 0.5$, $n = 5$, Fig. 2D) indicating that the channel is equally permeable to both Na^+ and K^+ . The results did not change whether voltage ramp protocols or voltage steps were used.

3.3. SmP2X has slow activation kinetics

Among the mammalian P2X subtypes, P2X1 and P2X3 display the fastest activation and desensitization kinetics whereas P2X2, P2X4 and P2X7 subunits generally show slower kinetics (Fig. 3A and see [1] for review). The activation kinetics of SmP2X mediated currents was dependent on the concentration of ATP (e.g. Fig. 2A). However at $100 \mu\text{M}$ ATP, SmP2X currents are significantly slower when compared to mammalian P2X currents (Fig. 3A). To compare the kinetics of activation among various P2X subtypes, the rise time of the ATP evoked currents, defined as the time required for the evoked response to reach from 10% to 90% of maximal response, was measured (Fig. 3B). P2X1 currents had the fastest rise time of 0.11 ± 0.003 s whereas P2X2 and P2X4 currents displayed slower kinetics with rise times of

1.3 ± 0.3 s and 1.10 ± 0.06 s, respectively (Fig. 3B). Under similar experimental conditions, SmP2X currents displayed the slowest activation kinetics with a rise time of 10 ± 1 s (Fig. 3B).

3.4. Submicromolar concentrations of zinc block SmP2X

Many ion channels including P2X receptors are sensitive to modulation by divalent cations such as zinc. Extracellular Zn^{2+} ions potentiate P2X2 (Fig. 4C) and P2X4 whereas they inhibit P2X7 responses [8–10]. Interestingly, specific NMDA subtypes of glutamate receptors are blocked by submicromolar concentrations of zinc [11]. We found that the co-application of zinc ions with the agonist ATP can effectively block the SmP2X mediated currents in a concentration dependent manner (Fig. 4A, B and D). The zinc blockade was reversible and exhibited a half-maximal concentration (IC_{50}) of $0.40 \pm 0.07 \mu\text{M}$ (Hill coefficient = 1.0 ± 0.2 , Fig. 4E). Similar results were obtained when zinc was applied prior to co-application with the agonist.

3.5. SmP2X exhibits pore dilation

Some vertebrate P2X subtypes dilate their pore during prolonged stimulation such that cations as large as 900 Da can pass through [12,13]. For example P2X7 mediates the passage of the cationic dye YO-PRO-1 (375 Da) which results in a change in the fluorescence property of the dye as it binds nucleic acids inside the cell. To determine the ability of SmP2X to mediate the uptake of large organic cations, oocytes expressing SmP2X, or

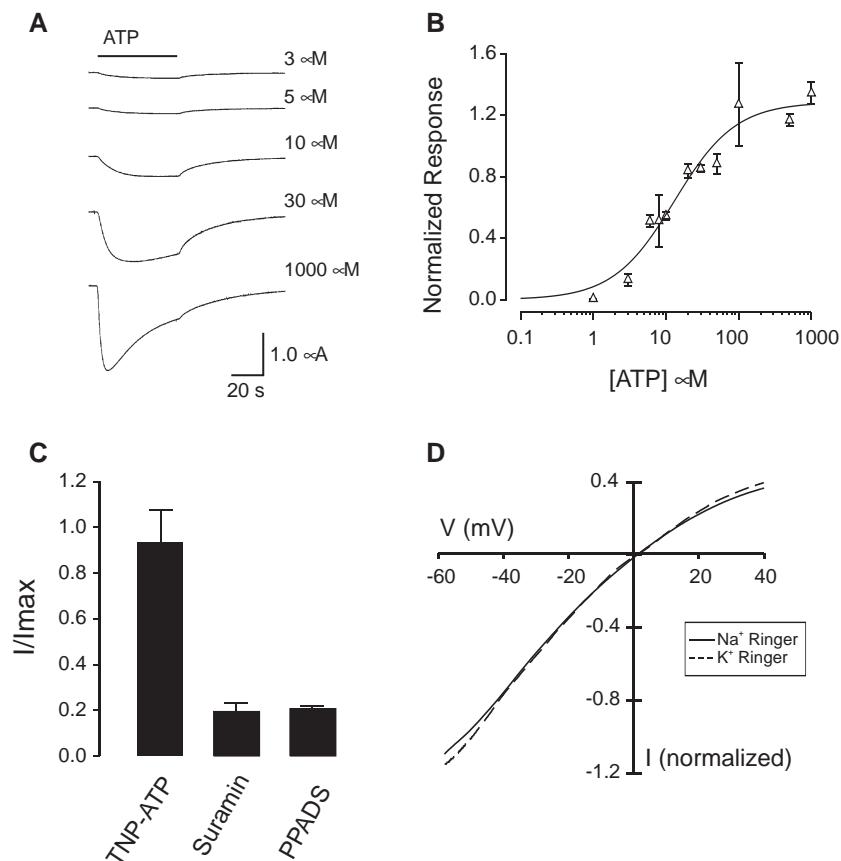


Fig. 2. Functional expression and characterization of SmP2X receptors in *Xenopus* oocytes. (A) Representative current responses of homomeric SmP2X receptors to different concentrations of ATP. (B) ATP dose-response relationship for SmP2X. Response at each concentration was normalized to the response to 100 μ M ATP. Each data point represents the normalized mean response of 3–10 oocytes. (C) Differential sensitivity of SmP2X to known P2X receptor antagonists. Current responses to 100 μ M ATP in the presence of each of the antagonists as a percentage of control (no antagonist) are plotted. Antagonists were pre-incubated for 5 min before co-application with ATP ($n=3-5$). (D) Ion permeation properties of SmP2X channels. Current-voltage (I-V) relationship for SmP2X obtained by voltage ramps in normal Ringer (solid line) or potassium Ringer (dashed line). The I-V curves are normalized to the current responses at -50 mV. The current traces are leak subtracted. Representative experiments ($n=5-6$) are shown.

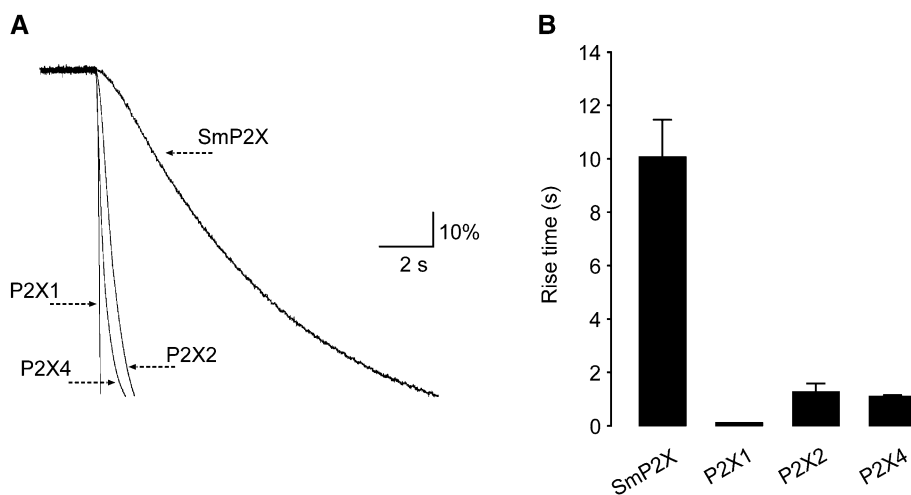


Fig. 3. SmP2X activation kinetics. (A) Representative current traces depicting the slower time course of ATP-mediated receptor activation in SmP2X, as compared to P2X1, P2X2, and P2X4 subtypes, are shown. Traces are normalized to the maximum response for each subunit. (B) The 10%-90% rise times are plotted for each homomeric P2X receptor ($n=3-6$).

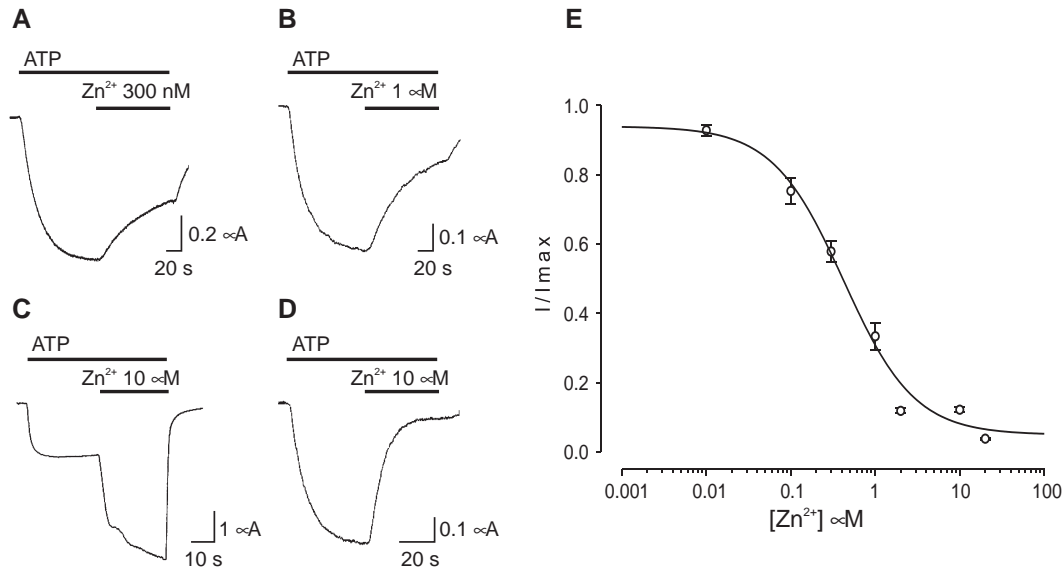


Fig. 4. Inhibition of SmP2X mediated currents by extracellular Zn²⁺ ions. (A and B) SmP2X currents in response to 5 μM ATP in the absence or presence of 300 nM and 1 μM zinc. (C and D) The opposite effect of 10 μM zinc on 5 μM ATP-evoked currents in oocytes expressing P2X2 (C) vs. SmP2X (D). (E) Dose-inhibition curve for the zinc inhibitory effect on SmP2X. Each data point is normalized to the control response (5 μM ATP) in the absence of zinc ($n=3-9$).

P2X7 as a positive control, were stimulated with ATP for 10 min in the presence of YO-PRO-1. Significant accumulation of the dye, as measured by increases in intracellular fluorescence intensity, was observed in oocytes expressing SmP2X or P2X7 following the stimulation (Fig. 5B, C and E). This indicates that SmP2X is also capable of pore dilation similar to mammalian P2X2, P2X4 and P2X7 receptors. Zinc could also effectively suppress pore dilation in SmP2X as YO-PRO-1 uptake was blocked in the presence of 20 μM zinc (Fig. 5D and E).

4. Discussion

In agreement with the recent report by Agboh et al. [5], the primary sequence of this two transmembrane domain protein from *S. mansoni* clearly identifies it as an invertebrate ATP-gated P2X receptor subunit. The mammalian P2X gene family encodes numerous subtypes with diverse functional properties. There is however only one P2X transcript identified in the *S. mansoni* EST data set—which currently encompasses 92% of the transcriptome [14]—hence there likely is only one P2X gene present in

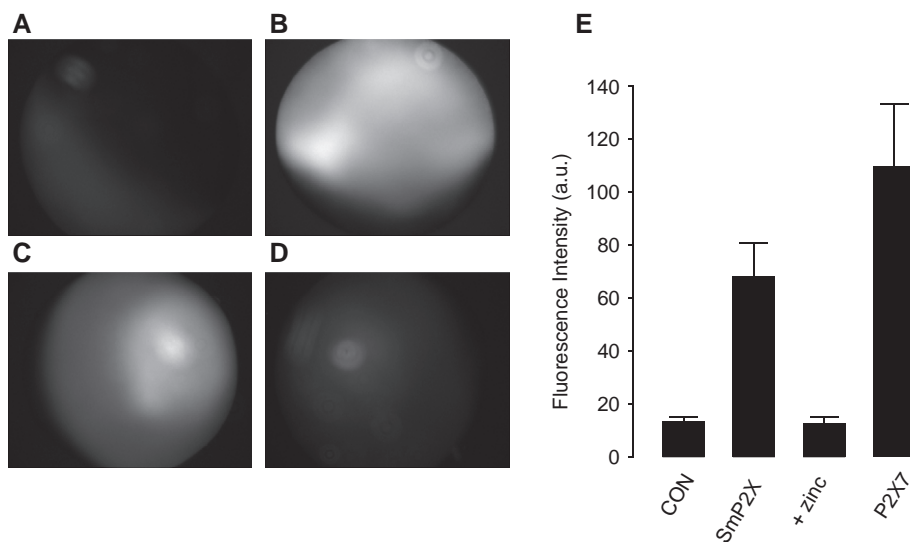


Fig. 5. SmP2X-mediated YO-PRO-1 uptake. (A) Oocyte expressing SmP2X incubated with YO-PRO-1 without ATP (control). (B) P2X7-expressing oocyte exposed to YO-PRO-1 and ATP (1 mM). (C) SmP2X-expressing oocyte incubated with YO-PRO-1 and ATP (100 μM) for 10 min. (D) Same as panel C but with 20 μM zinc. (E) Quantification of the fluorescence signals in dye uptake experiments. Intensities are reported in arbitrary units (a.u.) per unit area ($n=4-10$). CON, control.

the *Schistosoma* genome. Schistosomes belong to the order of platyhelminths which, along with annelids and mollusks, have branched off at the early stages of bilaterians evolution [15]. Therefore conserved genes present in *Schistosoma* may represent ancestors of mammalian genes [14]. This suggests that the sequence of Smp2X is closer to a common ancestral origin than any of the mammalian receptor subunits. The presence of functional ATP-gated channels in platyhelminths demonstrates also that nucleotides have been used early in the evolution as transmitters for fast intercellular communication.

It has been reported that codon usage or translation initiation may be an obstacle in expressing schistosome proteins in vertebrate heterologous expression systems [5,16]. Agboh and collaborators [5] have reported that alterations of the Smp2X cDNA were required for expression in *Xenopus* oocyte and HEK293 cells. However we found that no modifications of the sequences in the coding or untranslated regions were required for the functional expression of full-length Smp2X in *Xenopus* oocytes. ATP and BzATP are effective agonists for homomeric Smp2X receptors; however the receptor is not sensitive to $\alpha\beta$ ATP (at 100 μ M). Based on its agonist sensitivity profile, blockade by suramin and PPADS and insensitivity to TNP-ATP, Smp2X is functionally similar to mammalian P2X2 and P2X5 subtypes.

BzATP is a potent competitive blocker of several ATPases including those from primitive organisms such as yeast and thermophilic bacteria [17,18]. The sensitivity of Smp2X to BzATP reinforces the idea that the ATP binding site may have evolved from a common ancestor whereas sensitivity to $\alpha\beta$ ATP was acquired through mutations or gene duplications. The slow kinetics of Smp2X activation and desensitization suggests that fast-desensitizing P2X subtypes such as P2X1 and P2X3 may have evolved later during evolution by the acquisition of additional determinants and that the core primary structure of P2X receptors confers slow desensitization “by default”. The kinetic properties and the agonist profile of Smp2X receptor may also point to a structural link or a co-evolution between $\alpha\beta$ ATP sensitivity and fast desensitization.

We found that Smp2X can be significantly inhibited by zinc at submicromolar concentrations. Zinc positively modulates most vertebrate P2X subunits, with the exception of P2X7 which is inhibited by it. The half-maximal concentrations for the zinc effect range from 2 μ M at P2X2 to 20 μ M at P2X4 [19]. It inhibits P2X7 with a half maximal concentration of 10 μ M [9]. Smp2X possibly exhibits the highest sensitivity to zinc with a half-maximal concentration of 0.4 μ M, a value which is likely overestimated due to the presence of nanomolar concentrations of contaminating zinc in recording solutions in the absence of a chelator [11]. The reversible inhibition of Smp2X by zinc does not appear to be voltage dependent (IC_{50} values are similar at -60 and -120 mV, data not shown),

suggesting that open channel block is not the mechanism of inhibition. Zinc blockade was achieved during the application of ATP therefore Zn^{2+} ions can bind to the open state of the receptor-channel.

A hallmark of several vertebrate P2X subtypes is their change in ionic selectivity following activation. Oocytes expressing Smp2X exhibited significant YO-PRO-1 uptake after 10 min of ATP stimulation (Fig. 5). Hence pore dilation appears to be a property of the early ancestral ATP-gated channels. The function of such pore is not clear but P2X7-mediated pore formation has been shown to cause cytolytic cell death in immune cells [20,21]. Interestingly the Smp2X-mediated YO-PRO-1 uptake was significantly inhibited by zinc, suggesting that zinc binds to Smp2X in both channel and large pore conformations.

Smp2X defines a novel P2X subtype that despite low sequence homology, shares several functional properties with mammalian P2X2, P2X4, P2X5 and P2X7. Hence the comparison of Smp2X and vertebrate P2X sequences will facilitate the identification of common key residues involved in slow activation kinetics, pore formation and sensitivity to zinc blockade.

Schistosomiasis continues to be a major health problem in many tropical regions across the globe. Although effective, the current therapy with praziquantel is not available everywhere [22]. The exploitation of the high sensitivity of Smp2X to zinc blockade remains to be validated as a novel approach for the treatment of schistosomiasis (but see [23,24]), nevertheless the characterization of the molecular physiology of this human parasite will no doubt aid in the development of new treatments or methods of controlling its breeding.

Acknowledgements

The authors would like to gratefully acknowledge Marie-France Witty for technical assistance, Dr. Ariel Ase for helpful discussions, and Dr. Paula Ribeiro (McGill University) for providing the *Schistosoma* total RNA samples and cDNA library. R.R. is a CIHR Strategic Training Fellow in Pain: Molecules to Community. This work has been supported by a CIHR operating grant (P.S., MOP-14718). P.S. is a Killam Scholar.

References

- [1] R.A. North, Molecular physiology of P2X receptors, *Physiol. Rev.* 82 (2002) 1013–1067.
- [2] K.H. Backus, S. Braum, F. Lohner, J.W. Deitmer, Neuronal responses to purinoceptor agonists in the leech central nervous system, *J. Neurobiol.* 25 (1994) 1283–1292.
- [3] K.D. Clark, T.M. Hennessey, D.L. Nelson, External GTP alters the motility and elicits an oscillating membrane depolarization in *Paramecium tetraurelia*, *Proc. Natl. Acad. Sci. U. S. A.* 90 (1993) 3782–3786.

- [4] M.Y. Kim, H.G. Kuruvilla, S. Raghu, T.M. Hennessey, ATP reception and chemosensory adaptation in *Tetrahymena thermophila*, *J. Exp. Biol.* 202 (1999) 407–416.
- [5] K.C. Agboh, T.E. Webb, R.J. Evans, S.J. Ennion, Functional characterization of a P2X receptor from *Schistosoma mansoni*, *J. Biol. Chem.* 279 (2004) 41650–41657.
- [6] S. Verjovski-Almeida, R. DeMarco, E.A. Martins, P.E. Guimaraes, E.P. Ojopi, A.C. Paquola, J.P. Piazza, M.Y. Nishiyama Jr., J.P. Kitajima, R.E. Adamson, P.D. Ashton, M.F. Bonaldo, P.S. Coulson, G.P. Dillon, L.P. Farias, S.P. Gregorio, P.L. Ho, R.A. Leite, L.C. Malaquias, R.C. Marques, P.A. Miyasato, A.L. Nascimento, F.P. Ohlweiler, E.M. Reis, M.A. Ribeiro, R.G. Sa, G.C. Stukart, M.B. Soares, C. Gargioni, T. Kawano, V. Rodrigues, A.M. Madeira, R.A. Wilson, C.F. Menck, J.C. Setubal, L.C. Leite, E. Dias-Neto, Transcriptome analysis of the acoelomate human parasite *Schistosoma mansoni*, *Nat. Genet.* 35 (2003) 148–157.
- [7] R. Raouf, Y. Chakfe, D. Blais, A. Speelman, E. Boue-Grabot, D. Henderson, P. Seguela, Selective knock-down of P2X7 ATP receptor function by dominant-negative subunits, *Mol. Pharmacol.* 65 (2004) 646–654.
- [8] S.S. Wildman, B.F. King, G. Burnstock, Zn²⁺ modulation of ATP-responses at recombinant P2X2 receptors and its dependence on extracellular pH, *Br. J. Pharmacol.* 123 (1998) 1214–1220.
- [9] C. Virginio, D. Church, R.A. North, A. Surprenant, Effects of divalent cations, protons and calmidazolium at the rat P2X7 receptor, *Neuropharmacology* 36 (1997) 1285–1294.
- [10] K.T. Le, K. Babinski, P. Seguela, Central P2X4 and P2X6 channel subunits coassemble into a novel heteromeric ATP receptor, *J. Neurosci.* 18 (1998) 7152–7159.
- [11] P. Paoletti, P. Ascher, J. Neyton, High-affinity zinc inhibition of NMDA NR1-NR2A receptors, *J. Neurosci.* 17 (1997) 5711–5725.
- [12] B.S. Khakh, X.R. Bao, C. Labarca, H.A. Lester, Neuronal P2X transmitter-gated cation channels change their ion selectivity in seconds, *Nat. Neurosci.* 2 (1999) 322–330.
- [13] C. Virginio, A. MacKenzie, F.A. Rassendren, R.A. North, A. Surprenant, Pore dilation of neuronal P2X receptor channels, *Nat. Neurosci.* 2 (1999) 315–321.
- [14] S. Verjovski-Almeida, L.C. Leite, E. Dias-Neto, C.F. Menck, R.A. Wilson, Schistosome transcriptome: insights and perspectives for functional genomics, *Trends Parasitol.* 20 (2004) 304–308.
- [15] A. Adoutte, G. Balavoine, N. Lartillot, O. Lepinet, B. Prud'homme, R. de Rosa, The new animal phylogeny: reliability and implications, *Proc. Natl. Acad. Sci. U. S. A.* 97 (2000) 4453–4456.
- [16] F.F. Hamdan, A. Mousa, P. Ribeiro, Codon optimization improves heterologous expression of a *Schistosoma mansoni* cDNA in HEK293 cells, *Parasitol. Res.* 88 (2002) 583–586.
- [17] E. Vasilyeva, Q. Liu, K.J. MacLeod, J.D. Baleja, M. Forgac, Cysteine scanning mutagenesis of the noncatalytic nucleotide binding site of the yeast V-ATPase, *J. Biol. Chem.* 275 (2000) 255–260.
- [18] D. Bar-Zvi, M. Yoshida, N. Shavit, Modification of domains of alpha and beta subunits of F1-ATPase from the thermophilic bacterium PS3, in their isolated and associated forms, by 3'-O-(4-benzoyl)benzoyl adenosine 5'-triphosphate (BzATP), *J. Bioenerg. Biomembranes* 28 (1996) 471–481.
- [19] K. Xiong, R.W. Peoples, J.P. Montgomery, Y. Chiang, R.R. Stewart, F.F. Weight, C. Li, Differential modulation by copper and zinc of P2X2 and P2X4 receptor function, *J. Neurophysiol.* 81 (1999) 2088–2094.
- [20] F. Di Virgilio, P. Chiozzi, S. Falzoni, D. Ferrari, J.M. Sanz, V. Venketaraman, O.R. Baricordi, Cytolytic P2X purinoceptors, *Cell Death Differ.* 5 (1998) 191–199.
- [21] A. Surprenant, F. Rassendren, E. Kawashima, R.A. North, G. Buell, The cytolytic P2Z receptor for extracellular ATP identified as a P2X receptor (P2X7), *Science* 272 (1996) 735–738.
- [22] A. Fenwick, L. Savioli, D. Engels, N. Robert Bergquist, M.H. Todd, Drugs for the control of parasitic diseases: current status and development in schistosomiasis, *Trends Parasitol.* 19 (2003) 509–515.
- [23] H.N. Shi, M.E. Scott, K.G. Koski, M. Boulay, M.M. Stevenson, Energy restriction and severe zinc deficiency influence growth, survival and reproduction of *Heligmosomoides polygyrus* (Nematoda) during primary and challenge infections in mice, *Parasitology* 110 (Pt. 5) (1995) 599–609.
- [24] P. Kaestel, F.J. Lewis, A.L. Willingham, H.O. Bogh, L. Eriksen, K.F. Michaelsen, B. Sandstrom, C.E. Hoy, H. Friis, *Schistosoma japonicum* infection and serum and tissue concentrations of retinol and zinc in pigs, *Ann. Trop. Med. Parasitol.* 93 (1999) 489–499.